Seismic hazard mapping in Eugene-Springfield, Oregon

by Yumei Wang [1], David K. Keefer [2], and Zhenming Wang [1]

This paper was presented at the Seventh U.S.–Japan Workshop on Earthquake Disaster Prevention for Lifeline Systems, held November 4–7, 1997, in Seattle, Washington, and will be published in the Proceedings of that workshop by the National Institute of Standards and Technology, edited by Donald B. Ballantyne, EQE International, Seattle, Washington. We are publishing it here, with minor editorial changes, by permission of the authors. —*ed.*

ABSTRACT

The Oregon Department of Geology and Mineral Industries (DOGAMI) and the U.S. Geological Survey (USGS) are developing earthquake hazard maps for the Eugene-Springfield area in Lane County, Oregon. The method for producing the map is derived from state-of-practice dynamic analyses for ground-response, slope-stability, and liquefaction analyses; empirical correlations of slope stability with engineering properties of materials; and manipulation of data on local topography, engineering geology, and hydrology, using geographic information system (GIS) tools. Specific types of data used to produce the map include (1) distribution of geologic units, (2) engineering properties of materials in each geologic unit, (3) slope inclinations, (4) regional hydrology, (5) distribution of existing landslide deposits, (6) distribution of artificial slope alterations, and (7) ground motions from design scenario earthquakes (M 6.5 shallow crustal and M 8.3 subduction zone event).

Seismically induced ground deformation is evaluated as follows: Slopes steeper than 25° are analyzed using empirical criteria that relate slope stability to degree of weathering, strength of cementation, spacing and openness of rock fractures, and hydrologic conditions. Slopes between 5° and 25°, which in the project area are commonly mantled with aprons of heterogeneous colluvium, are evaluated with a dynamic slope-stability analysis that uses slope inclinations, engineering geologic characteristics of geologic units, and shaking parameters from design earthquakes as inputs. Slopes gentler than 5° are analyzed for liquefaction and resultant lateral spreading. Results of these analyses are then combined to produce a ground deformation map with five slope instability categories (very high, high, medium, low, and nil potential for slope failure). Site periods and maximum spectral ratio are also shown on the ground deformation hazards map. Site effects of local geology on ground shaking are evaluated using the program SHAKE91. Site periods and maximum amplification of spectral accelerations are determined and used to produce a ground response map.

The 1:24,000-scale maps resulting from this study are intended for use by local communities for regional planning and mitigation purposes. Techniques developed in this study are intended to be applicable to regional-scale mapping in other areas with a wide variety of topographic, geologic, and hydrologic characteristics.

INTRODUCTION AND PURPOSE

Many types of earthquake hazards can be evaluated and mitigated to an acceptable level of risk in advance of future damaging earthquakes. Ground failures from slope instability can be a significant threat, especially in urban areas with concentrated development on unstable slopes. Amplified ground shaking can be destructive, intensifying and prolonging ground shaking. Many recent earthquakes have caused significant loss of life and property damage from earthquake-induced landslides and amplified ground shaking.

This paper presents a preliminary method for producing an earthquake hazard map showing (1) dynamic (i.e., earthquake-induced) slope stability for slopes that range from steep to gentle, and (2) dynamic ground response. Dynamic slope stability is evaluated for a wide spectrum of landslide failure types. Steep slopes (>25°) are most susceptible to rockfalls and other fast-moving landslides; moderate slopes (5°–25°) are susceptible to deep-seated rotational and translational block slides; and even gentle slopes (<5°) may be susceptible to liquefaction-induced lateral spreading. Ground response results show site periods and maximum spectral ratio (earthquake-related engineering properties of a site). Site periods and maximum spectral ratios are shown as 0.1-second and 1.0-contour intervals, respectively.

The method described here for producing a hazard map is derived from dynamic ground-response, slope-stability, and liquefaction analyses; empirical correlations of slope stability with engineering properties of materials; and manipulation of data on local topography, engineering geology, and hydrology, using geographic information system (GIS) tools. The final map will be produced at a scale of 1:24,000 and with 30-ft-grid digital elevation model (DEM) data and will provide information for regional planning, design, and mitigation. The map should serve as a useful tool in

[1] Oregon Department of Geology and Mineral Industries, 800 NE Oregon St., #28, Portland, OR 97232, USA
[2] U. S. Geological Survey, 345 Middlefield Rd., MS 977, Menlo Park, CA 94025, USA

reducing hazards through effective land-use and emergency planning, regional vulnerability studies, identification of areas that would benefit from site-specific studies, and organization of mitigation efforts.

The project area encompasses three 7½-minute quadrangles (Eugene West, Eugene East, and Springfield) and totals about 200 mi^2 (Figure 1). The project area is rectangular, includes the Metro Plan boundary, and extends beyond the three quadrangles. This project involves working closely with an advisory task force composed of local community members. It also includes establishing a temporary local seismograph network to monitor local and distant earthquakes to gain a better understanding of local sources and ground response, and performing an evaluation of structural seismic vulnerability on a limited number of selected buildings.

BACKGROUND

From beginnings in the 1840s, the population of the Eugene-Springfield metropolitan area is now approaching 200,000 and continues to increase. The population within the Metro Plan boundary (Figure 1), an area slightly larger than both the city and urban growth areas, is projected to increase by approximately 57 percent between 1990 and 2020 (Meacham, 1990).

Building expansion continues to penetrate the hillslope and urban development areas, which tend to be difficult areas for building. Due to the nature of the geology, topography, and climate, certain areas are prone to ground failure and amplified ground shaking, which threaten both existing and new developments.

Geographic setting

The project area is located in the southern reach of the upper Willamette basin near the confluence of the Coast and Middle Fork Willamette Rivers and the McKenzie River. It includes hills bounding the valley, with the Cascades on the east flank and the Coast Range on the west and south. The climate is moderate in temperature, and the average annual precipitation is 40 in. Generally, the elevation of central Eugene and Springfield is about 400 ft.

Geologic setting

The Willamette Valley geomorphic province is a broad lowland separating the Oregon Coast Range from the Cascade Range. This terrain is part of the forearc basin associated with the Cascadia subduction zone and consists of interfingering, gently dipping Tertiary rocks ranging from Eocene to Miocene in age,

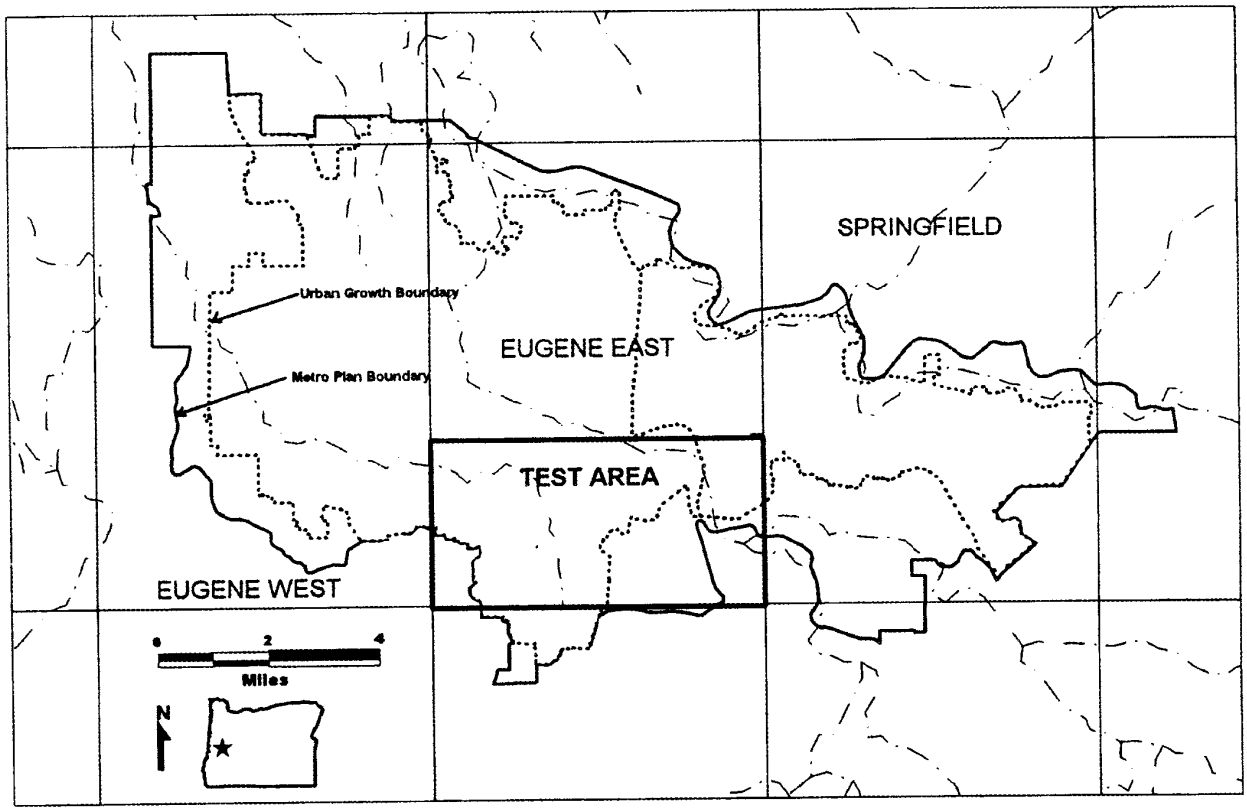

Figure 1. Location map showing test area for pilot project and its location with respect to urban growth and Metro Plan boundaries of the Eugene-Springfield area as well as main topographic quadrangles. Dash-dot lines mark major drainages.

including volcanic flows and intrusions, tuffaceous sediments, and sedimentary rocks (Walker and Duncan, 1989). In the Willamette Valley, bedrock units are overlain by Quaternary-age alluvium and thus are not well understood in detail. The smooth alluvial plain of the Willamette Valley is interrupted by occasional flood and stream channels. Table 1 describes the geologic units found, and Figure 2 shows their distribution, in the test area that is discussed later under "Slope Analyses."

Seismic setting

The physiographic setting of the Pacific Northwest results from its plate tectonic setting. From northern California to British Columbia, oceanic plates, including the Juan de Fuca plate, are being subducted beneath the North American plate along the Cascadia subduction zone. Earthquakes can occur within the subducting Juan de Fuca plate (oceanic intraplate earthquakes), within the overriding North American plate (crustal earthquakes), or along the interface between the two

Table 1. *Geologic units in the Eugene-Springfield metropolitan area. Modified from Walker and Duncan (1989).*

Symbol	Age	Description
Qal	Holocene	**Alluvium**—Clay, silt, sand, and gravel in river and stream channels
Qoal	Holocene/Pleistocene	**Older alluvium**—Poorly consolidated clay, silt, sand, and gravel marginal to active stream channels and filling lowland plains of Willamette River Basin and tributary drainages
Tub	Miocene	**Basalt and basaltic andesite flows and flow breccias**—Grades laterally into palagonitic tuff and breccia and into clastic sedimentary rocks
Ti	Oligocene	**Mafic intrusions**—Sheets, sills, and dikes of massive granophyric ferrogabbro; some bodies strongly differentiated and include pegmatitic gabbro, ferrogranophyre, and granophyre
Tf	Oligocene/Eocene	**Fisher Formation, undivided**—Predominantly continental volcaniclastic rocks, including andesitic lapilli tuff, breccia, water-laid and air-fall silicic ash, and interbedded basaltic flows
Te	Oligocene/Eocene	**Eugene Formation**—Thin- to moderately thick-bedded, coarse- to fine-grained arkosic, micaceous, and, locally, palagonitic sandstone and siltstone, locally highly pumiceous, assigned to the upper Eocene to middle Oligocene, marine Eugene Formation
Tfb	Eocene	**Basaltic flows**—Flows, some of which may be invasive into the undivided Fisher Formation (unit Tf), and undivided and questionable sills that may intrude the undivided Fisher Formation

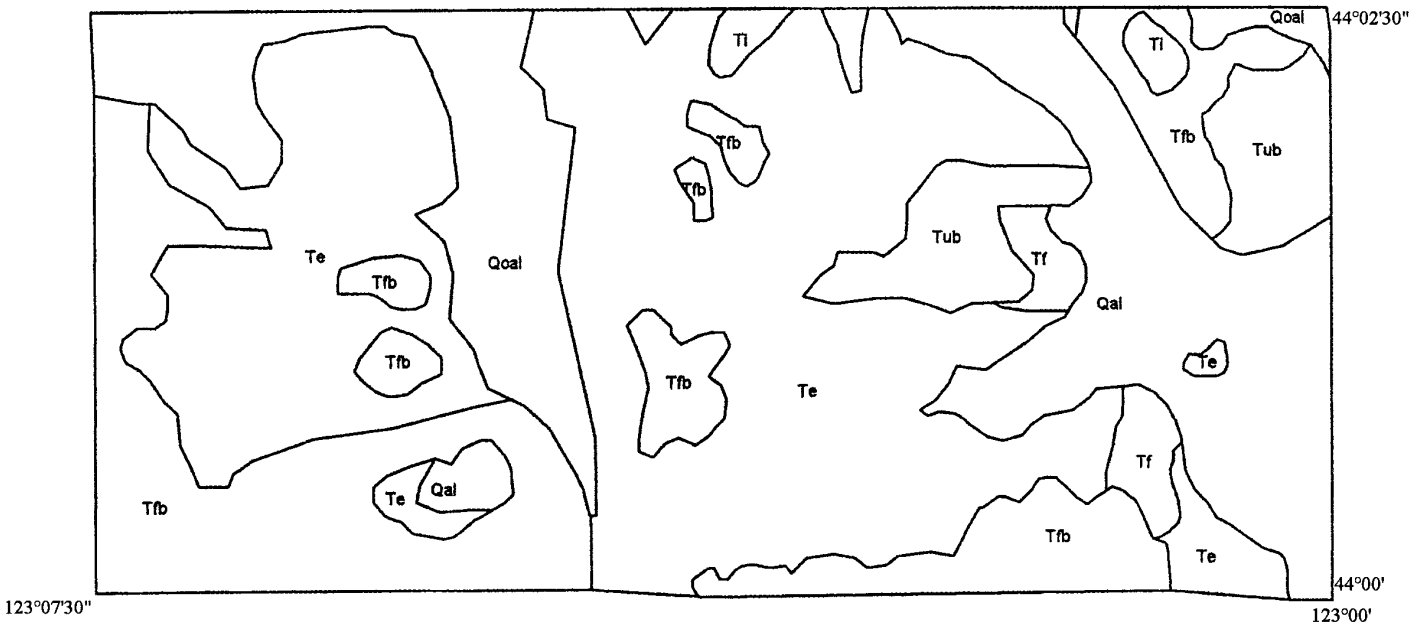

Figure 2. Simplified geologic map of test area, modified from Walker and Duncan (1989). Coordinates approximate. Geologic unit symbols keyed to Table 1 above.

plates (subduction zone earthquakes). All three possible earthquake types (subduction, oceanic intraplate, and crustal) can severely impact the project area, and each was considered as part of this study.

Although no damaging earthquakes have occurred during historic times, small local earthquakes have been recorded. A recent study that focused on evaluating ground response in Eugene and Springfield (R. Weldon and S. Perry-Huston, University of Oregon Geological Sciences Department, unpublished data) included the recording of several very small local earthquakes. In January 1996, a cluster of small earthquakes occurred about 15 mi east of Eugene. Later, in May 1996, a small earthquake occurred about 3 mi north-northwest of downtown Eugene. These earthquakes have not been identified with any specific fault structure (S. Perry-Huston, oral communication, 1997) but indicate zones of potential threat to local communities. The project area is located about 60 mi east of the Cascadia subduction zone, where several large-magnitude subduction zone earthquakes are thought to have occurred in the past few thousand years (Atwater, 1996). A strong local crustal earthquake or great subduction zone earthquake would likely produce strong ground shaking for all geologic units in the project area. Bedrock ground motions incorporated in the study were developed by Geomatrix Consultants, Inc. (1995).

DATA COLLECTION

The method used to evaluate earthquake-induced ground failure and local ground response requires information on the geologic units (their distribution and engineering characteristics), slope angles, hydrology, and the occurrence of existing landslides and large artificial slope alterations. The distribution of geologic units was determined from published geologic maps (Walker and Duncan, 1989; Vokes and others, 1951) and from additional mapping carried out as part of the study. The engineering properties of materials in each geologic unit were determined from field mapping, laboratory testing of selected materials, in situ tests, and engineering judgment. Field work included the mapping of over 200 outcrops considered to be reasonably representative of the geologic units. In situ tests included downhole shear wave velocity profiling, surface refraction profiling, and standard penetration testing. Slope inclinations were determined using geographic information system (GIS) tools and digital elevation models (DEMs) with a grid spacing of 30 ft. Regional hydrology was determined from borehole and well data, mapping of springs and seeps, and also hydrologic modeling conducted by the local water departments. Existing landslide deposits were mapped as part of the study. Input on active landslides was provided by local consultants and public works department staff. Lastly, artificial slope alterations, such as large road and railroad cuts were identified. The method does not specifically address slope aspect, vegetation, and human effects (such as logging and grading practices).

SLOPE ANALYSES

Preliminary analyses were conducted in a test area that covers about 20 mi^2 of the project area (Figure 1). Slopes in the test area are divided into four groups: (A) existing landslides; (B) steep slopes, greater than 25°; (C) moderate slopes, ranging from 5° to 25°; and (D) gentle slopes, less than 5° (Figure 3). It was assumed that groups (B), (C), and (D) have fundamentally different modes of dynamic failure. Consequently, different analytical techniques were applied to these groups as shown in Figure 4.

(A) Existing landslides

The movement characteristics of existing landslides are highly variable and range from actively moving to stable. To understand the nature of each existing landslide would require numerous site-specific evaluations. In the absence of this landslide information, it was assumed that the slip planes are at reduced shear strengths of unknown values, and that existing landslide masses are inherently unstable under earthquake loading. Thus, existing landslides were assigned to the very high susceptibility rating. No analytical techniques were applied.

(B) Steep slopes

Bedrock slopes greater than 25° are particularly susceptible to slope failures (Keefer, 1993). Consequently, slopes greater than 25° were assigned to Group B, steep slopes. Engineering properties of geologic units, including degree of weathering, strength of cementation, spacing and openness of rock fractures, and hydrologic conditions, were mapped in outcrops. Each outcrop was assigned to a mapped geologic unit. Then, each geologic unit was evaluated for susceptibility to slope failure, using a decision tree outlined in Keefer (1993) and shown in Figure 5.

For each geologic unit, the average value from the rating category was analyzed, using empirical criteria that relate slope instability to area (Keefer, 1993). Keefer (1993) related engineering properties observable in outcrop to landslide concentrations, expressed as number of landslides per square kilometer (LS/km^2) (1 $km^2 \approx 0.4$ mi^2). For the geologic units within the test area, each outcrop was rated according to Figure 5. Then, the results were averaged for each geologic unit, using the following landslide concentration relationship:

$$LS/km^2 = (32)(\%\text{ extremely high}) + (8)(\%\text{ very high}) + (2)(\%\text{ high}) + (0.125)(\%\text{ low}),$$

where the multipliers (32, 8, 2, and 0.125) are taken from landslide concentrations used to assign ratings in Keefer (1993). Landslide concentration results are

shown in Table 2, column 3. Then, each geologic unit was assigned a new susceptibility rating compatible with the DOGAMI earthquake hazard rating system of high, medium, or low on the basis of calculated landslides per square kilometer value as follows:

high > 2 LS/km^2 > medium
> 1 LS/km^2 > low.

Table 2. *Landslide concentration and ratings for geologic units. Geology after Walker and Duncan (1989)*

	Geologic unit	Lithology	LS/km^2	DOGAMI rating
Tfb	Basalt flows	Basalt	10.82	High
Te	Eugene Formation	Sandstone	5.34	High
Tf	Fisher Formation	Volcaniclastics	2.73	High
Tub	Basalt flow breccias	Breccias	1.83	Medium
Ti	Mafic intrusions	Gabbro	1.30	Medium

The resulting dynamic landslide susceptibilities for each geologic unit are shown in Table 2, column 4.

The following illustrates how the susceptibility was determined for a specific geologic unit, unit Tub, which consists predominantly of basalt and basaltic andesite flows and flow breccias: A total of 34 outcrops was mapped and evaluated in accordance with Keefer's (1993) method. Of this total, 31 outcrops, or 91 percent, were assigned a susceptibility rating of high, and 3 outcrops, or 9 percent, were assigned a rating of low. Landslide concentration was determined as follows:

$$2 \times 0.91 + 0.125 \times 0.09 = 1.83$$

and produced a result of 1.83 landslides per square kilometer. This value falls into the medium susceptibility rating.

(C) Moderate slopes

Slopes ranging from 5° to 25° were assigned to Group C, moderate slopes. For moderate slopes, we assumed that coherent, relatively deep-seated translational and rotational slides are the most common modes of failure (Keefer, 1984). Moderate slopes in the project area are commonly mantled with aprons of heterogeneous colluvium. Our method for rating these slopes is based on the dynamic slope stability analysis of Newmark (1965), as verified and extended to regional-scale use by Wilson and Keefer (1983, 1985), Wieczorek and others (1985), Jibson (1993, 1996), and Jibson and Keefer (1993).

The selected earthquake input parameters included two controlling events: A magnitude 8.5 subduction zone earthquake at a 100-km (~60-mi) distance from

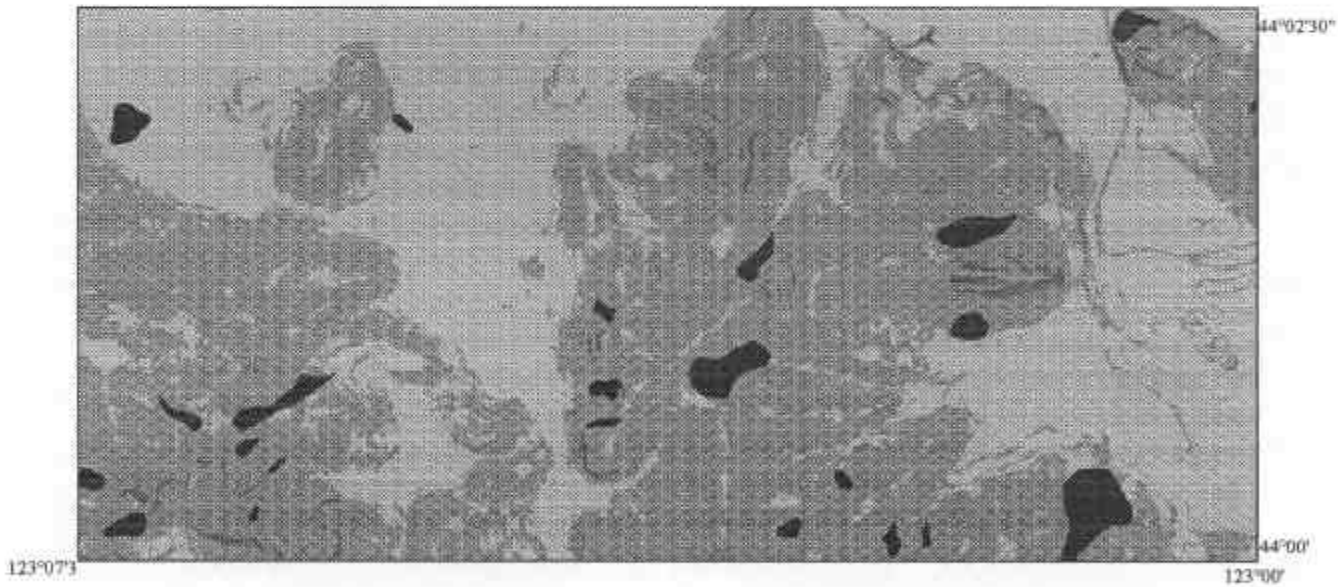

Figure 3. Distribution of slope types—groups A, B, C, and D—in test area (approximately, bottom third of Eugene East quadrangle). Different analytical techniques were applied to these groups.

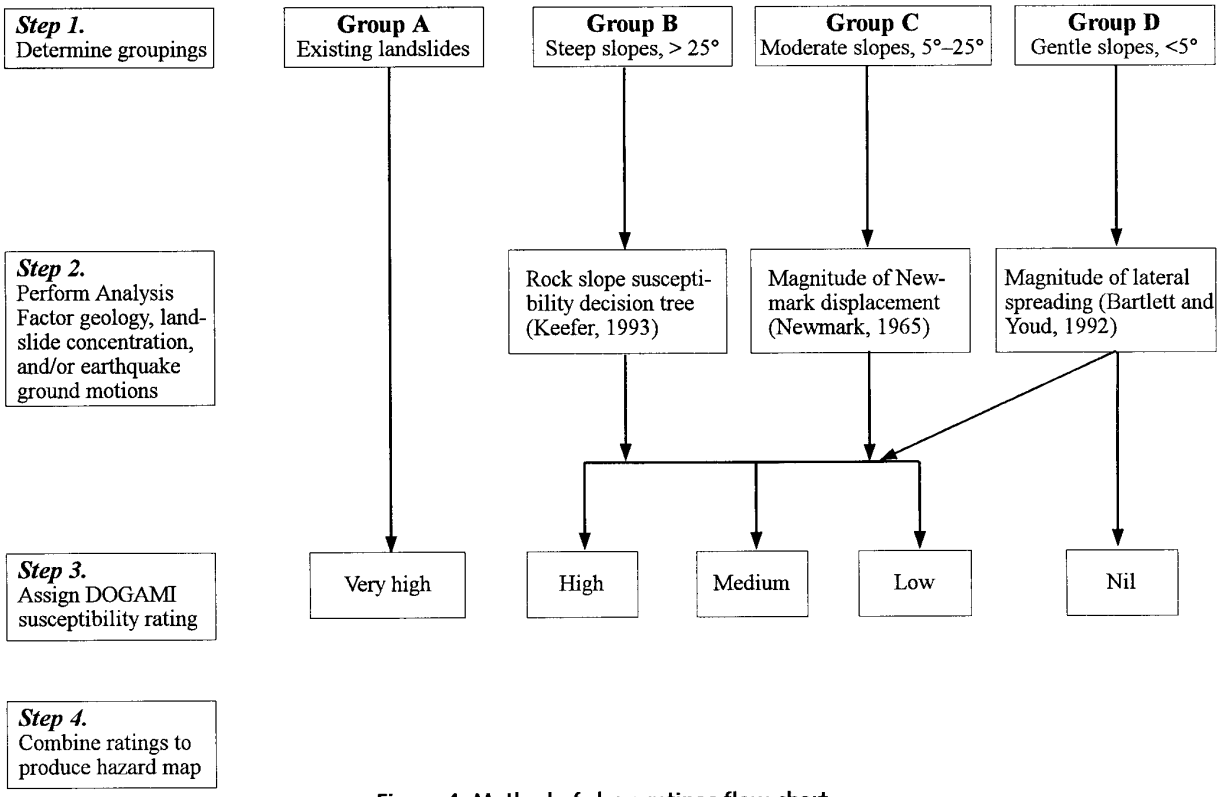

Figure 4. Method of slope ratings flow chart.

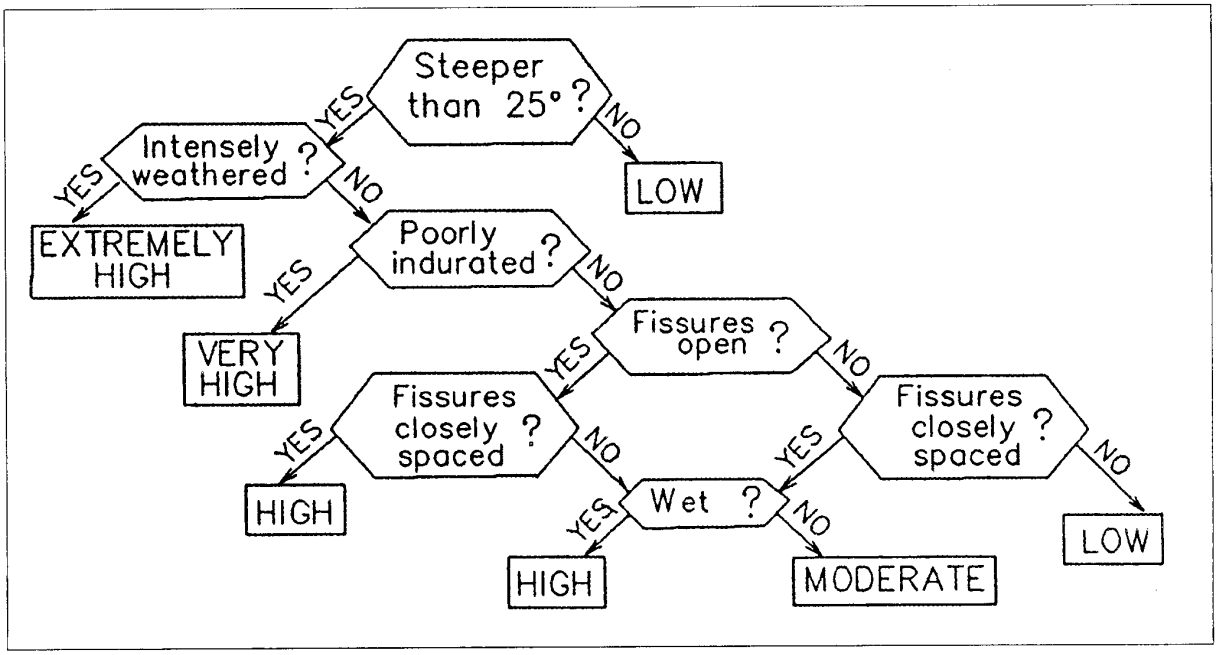

Figure 5. Decision tree for susceptibility of rock slopes to earthquake-induced landslides (from Keefer, 1993). For the test area, all slopes were assumed to be wet.

the earthquake source and a magnitude 6.5 event at 10-km (~6-mi) distance. Arias Intensity (I_a) values were determined based on magnitude and distance from the source according to the equation developed by Wilson and Keefer (1985):

$$\log (I_a) = \mathbf{M} - 2 \log R - 4.1,$$

where I_a is in meters per second, **M** is moment magnitude, and R is earthquake source distance in kilometers. Next, assuming an infinite slope failure, an equation by Newmark (1965),

$$a_c = (FS - 1)\, g \sin \alpha,$$

was used to calculate the critical acceleration (a_c). Here, a_c is the acceleration required to overcome frictional resistance and initiate sliding in terms of g, the acceleration due to Earth's gravity; FS is the static factor of safety; and α is the angle from the horizontal by which the center of the mass of the potential landslide block first moves. The Newmark displacement (D_N, in cm) was then determined from the relationship (Jibson, 1993; Jibson and Keefer, 1993):

$$\log (D_N) = 1.460 \log I_a - 6.642\, a_c + 1.546.$$

Finally, each slope was assigned a DOGAMI susceptibility rating based on the calculated displacement D_N:

high > 100 cm > medium > 10 cm > low,

as shown in Figure 4.

(D) Gentle slopes

Slopes less than 5° were assigned to Group D, gentle slopes. For these, we calculated lateral-spreading (i.e., slope-instability) susceptibility for Quaternary-aged geologic units that are prone to liquefaction failure. Gentle slopes underlain by pre-Quaternary geologic units were assumed to be stable and were automatically given a susceptibility rating of nil. Areas of Quaternary-aged units were separated in order of depositional age, with artificial fill and the youngest deposits generally being the most vulnerable to slope movement. The selected earthquakes include a **M** 6.5 event at a 10-km distance and a **M** 8.5 subduction zone earthquake at a 100-km (~60-mi) distance and were adopted from an Oregon Department of Transportation study (Geomatrix Consultants, Inc., 1995).

To evaluate for lateral-spreading susceptibility, we first estimated the site effects of local geology on ground shaking by using SHAKE91, a commercially available program for analyzing one-dimensional site-response of vertically propagating (normally incident) shear waves at a level site (Idriss and Sun, 1992). Peak rock accelerations on the synthetic acceleration time history were scaled to 0.34 g and used as input parameters in SHAKE91. The peak surface accelerations determined from SHAKE91 analysis were used as input accelerations in the liquefaction analyses.

Next, initial liquefaction was analyzed by two methods: The first, by Robertson and Fear (1996), is an improvement of the method developed by Seed and others (1984) and is based on standard penetration test (SPT) measurements. The second, by Andrus and Stokoe (1996), is based on shear wave velocity measurements. Both methods were used to maximize the available in situ data in the project area and account for the uncertainties associated with evaluating the predominantly gravelly soils.

For soils that are prone to liquefaction, lateral spreading was estimated using Barlett and Youd (1992). According to Barlett and Youd (1992), lateral spreading due to liquefaction satisfies:

$$\log (D_H) = -15.787 + 1.178\, \mathbf{M} - 0.927 \log R - 0.013\, R + 0.429 \log S + 0.348 \log T_{15} + 4.527 \log (100 - F_{15}) - 0.922\, D50_{15},$$

where D_H is lateral spreading in meters; **M** is moment magnitude; R is horizontal distance to the nearest seismic energy source, in kilometers; S is ground slope, in percent; T_{15} is the cumulative thickness, in meters, of saturated cohesionless soils with $(N_1)_{60}$ value ≤15; F_{15} is the average fines content, in percent; $D50_{15}$ is mean grain size.

To illustrate this method, we used drill hole data from Test Site ES-2, which is located in the Eugene West quadrangle (Figure 1). SHAKE91 was run, and a peak surface acceleration of 0.40 g was achieved. Liquefaction was analyzed using methods of Robertson and Fear (1996) and Andrus and Stokoe (1996). Next, for soils that liquefy, lateral spreading was calculated, using Bartlett and Youd (1992). We assumed: **M** = 8.5, R = 100 (km), $D50_{15}$ = 1.0 (mm), F_{15} = 5 percent, T_{15} = 5 m, and S ranging from 1° to 5°. Results, shown in Table 3, indicate that for this liquefiable deposit, steeper slopes have greater lateral spreading displacements (0.56 m) than gentler slopes (0.28 m). According to the method shown in Figure 4, the DOGAMI susceptibility rating based on the calculated displacement D_H,

high > 100 cm > medium > 10 cm > low — or nil,

places all of these slopes in the medium susceptibility category.

Table 3. *Lateral spreading displacements (D_H) for test site ES-2. After Bartlett and Youd (1992)*

Slope (S, in degrees)	Displacement (D_H, in meters)
1	0.28
2	0.38
3	0.45
4	0.51
5	0.56

Slope susceptibility ratings

Applying susceptibility ratings within each of the four groups (A—existing landslides, B—steep slopes, C—moderate slopes, and D—gentle slopes) requires professional judgment. The last step involves bringing the independent analytical results from each group together to produce a coherent, uniform, relative hazard susceptibility map. Results from each group fall within one of five susceptibility ratings for dynamic slope instability: very high, high, medium, low, and nil (Figure 4).

DYNAMIC GROUND RESPONSE ANALYSES

For the local geologic conditions in valley areas with about 10 ft or more of soil deposits (Figure 6), site period and maximum spectral ratio were evaluated. Site effects on ground shaking were determined using SHAKE91. Design earthquakes for M 6.5 crustal and M 8.3 subduction zone events were modeled, assuming epicentral distances of 10 km and 100 km, respectively.

Preliminary results of site period, which was determined for 26 site-specific soil locations, were contoured at 0.1-second intervals (Figure 7). At these locations, amplification curves and Fourier response spectra were plotted to determine maximum spectral ratios, that is, maximum amplification of spectral accelerations. Figure 8 illustrates the process of determining maximum spectral ratios, including the input parameters (initial damping, density, shear wave velocity), input and output acceleration time histories, and spectral response showing the maximum spectral ratios. Figure 9 shows preliminary results of maximum spectral amplification contours. These amplification factors can be correlated with site period (shown in Figure 7) to indicate areas of potential soil-structure resonance that can cause structural damage. Higher damage also occurs in areas with prolonged strong shaking, which can be generally related to areas with longer site periods.

DISCUSSION

The method described in this paper is still under development, and preliminary results using this method are scheduled to undergo additional review during 1998. The tentative final product is one 1:24,000-scale colored map showing ground failure hazards, site period, and maximum spectral ratios. These data were selected by community representatives with the assistance of DOGAMI and USGS staff for the purpose of predicting high-damage areas for a wide range of users.

Additional research is needed to improve the accuracy of predicting dynamic ground response on a regional basis. To calibrate the reliability of this method, more post-earthquake field calibrations must be performed. Special attention should be given to determining dynamic slope-stability hazards for moderate slopes.

ACKNOWLEDGMENTS

We owe special thanks to Stephen E. Dickenson of the Oregon State University Civil Engineering Department and Robert E. Kayen of the U.S. Geological Survey for their helpful reviews. We also thank Gerald Black for technical advice, Donald Hull and John Beaulieu for supporting this study, Klaus Neuendorf for editorial assistance, Tom Wiley and Robert Murray for geologic assistance, and Neva Beck for assisting in the preparation of this paper.

REFERENCES CITED

Andrus, R.D., and Stokoe, K.H., 1996, Guidelines for evaluation of liquefaction resistance using shear wave velocity: Paper presented at NCEER Workshop on Evaluation of Liquefaction Resistance, Jan. 4–5, 1996, Salt Lake City, Utah.

Atwater, B.F., 1996, Coastal evidence for great earthquakes in western Washington, in Rogers, A.M., Walsh, T.J., Kockelman, W.J., and Priest, G.R., eds., Assessing earthquake hazards and reducing risk in the Pacific Northwest: U.S. Geological Survey Professional Paper 1560, v. 1, p. 75–90.

Bartlett, S.F., and Youd, T.L., 1992, Empirical prediction of liquefaction-induced lateral spread: Journal of Geotechnical Engineering, v. 121, no. 4, p. 316–329.

Geomatrix Consultants, Inc., 1995, Seismic design mapping, State of Oregon: Final report to Oregon Department of Transportation, Project no. 2442, var. pag.

Idriss, I.M., and Sun, J., 1992, User's manual for SHAKE 91, a computer program for conducting equivalent linear seismic response analyses of horizontally layered soil deposits: Unpublished report sponsored by National Institute of Standards and Technology, Building and Fire Research Laboratory, Structures Division, Gaithersburg, Maryland, and University of California at Davis, Department of Civil and Environmental Engineering, Center for Geotechnical Modeling, Davis, Calif., var. pag.

Jibson, R.W., 1993, Predicting earthquake-induced landslide displacements using Newmark's sliding block analysis: Washington, D.C., National Research Council Transportation Research Record 1411, p. 9–17.

———1996, Use of landslides for paleoseismic analysis: Engineering Geology, v. 43, p. 291–323.

Jibson, R.W., and Keefer, D.K., 1993, Analysis of the seismic origin of landslides: Examples from the New Madrid seismic zone: Geological Society of American Bulletin, v. 105, no. 4, p. 521–536.

Keefer, D.K., 1984, Landslides caused by earthquakes: Geological Society of America Bulletin, v. 95, no. 4, p. 406–421.

———1993, The susceptibility of rock slopes to

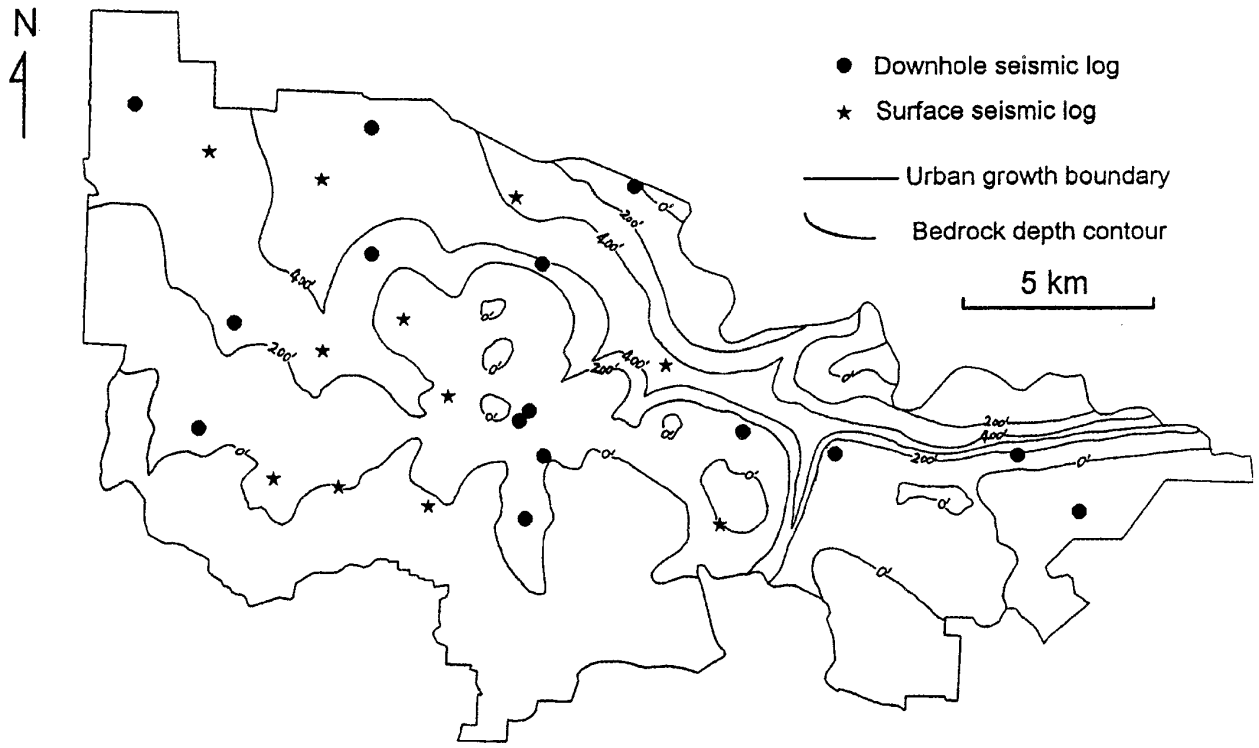

Figure 6. Location of seismic log and generalized depth to bedrock contours in the Eugene-Springfield urban growth boundary. Contours in 200-ft intervals.

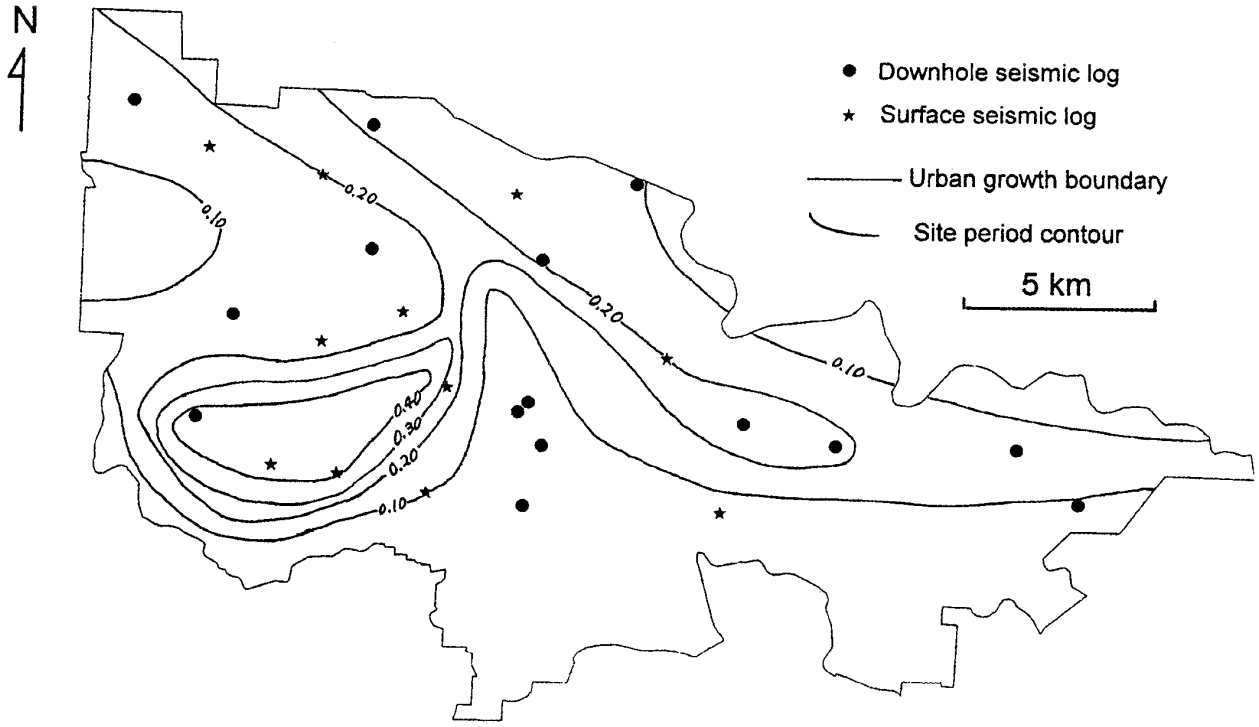

Figure 7. Site period, preliminary results. Contours in 0.1-second intervals.

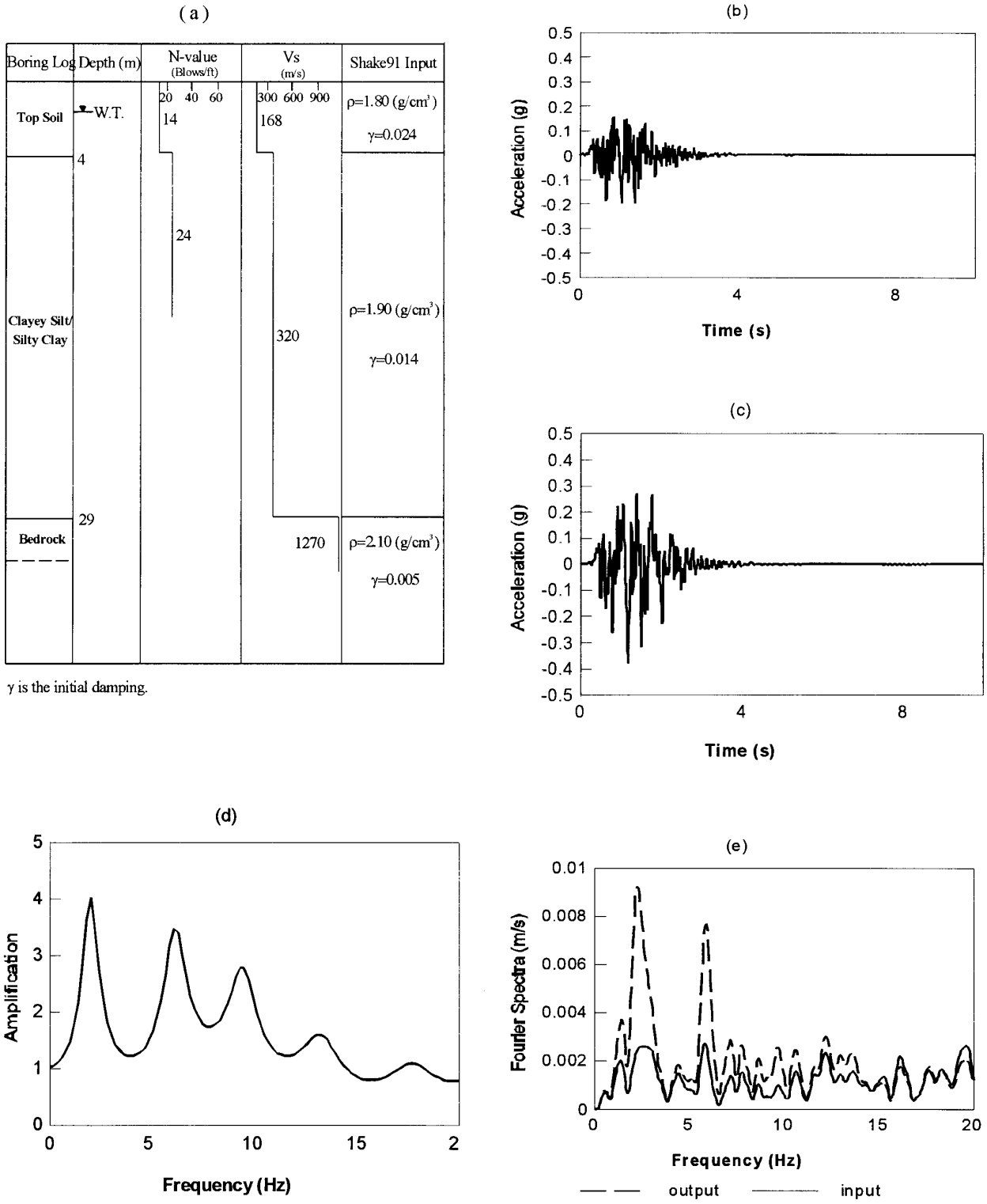

Figure 8. Soil column and SHAKE91 modeling at Site ES-2. (a) soil column and SHAKE91 input parameters; (b) input ground motion (M 6.5 crustal earthquake) at bedrock; (c) output ground motion on free surface; (d) amplification curve; (e) input and output Fourier spectra.

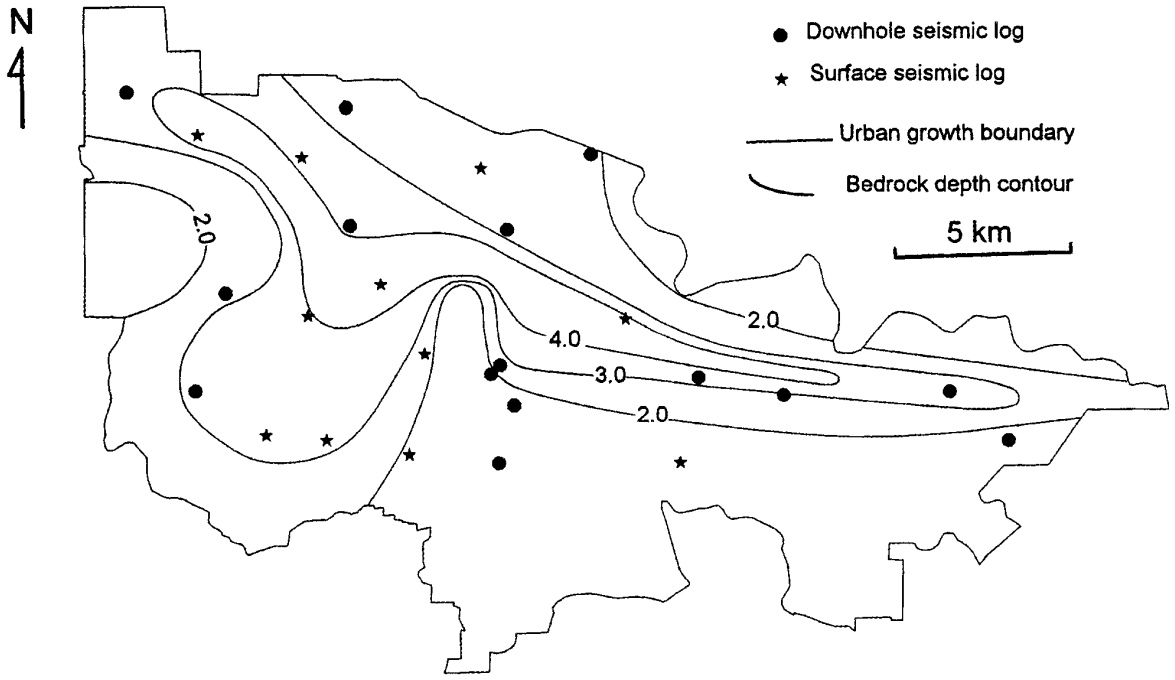

Figure 9. Spectral amplification, preliminary results. Contours in 1.0 intervals.

earthquake-induced failure: Association of Engineering Geologists Bulletin, v. 30, no. 3, p. 353–361.

Meacham, J.E., ed., 1990, Atlas of Lane County, Oregon: Eugene, Oreg., QSL Printing Company, 73 p.

Newmark, N.M., 1965, Effects of earthquakes on dams and embankments: Géotechnique, v. 15, no. 2, p. 139–159.

Robertson, P.K., and Fear, C.E., 1996. Soil liquefaction and its evaluation based on SPT and CPT: Paper presented at NCEER Workshop on Evaluation of Liquefaction Resistance, Jan. 4–5, 1996, Salt Lake City, Utah.

Seed, H.B., Tokimatsu, K., Harder, L.F., and Chung, R.M., 1984, The influence of SPT procedures in soil liquefaction resistance evaluations: Berkeley, Calif., University of California, College of Engineering, Earthquake Engineering Research Center Report UCB/EERC–84/15, 50 p.

Vokes, H.E., Snavely, P.D., and Myers, D.A., 1951, Geology of the southern and southwestern border areas of the Willamette Valley, Oregon: U.S. Geological Survey Oil and Gas Investigations Map OM–110, scale 1:62,500.

Walker, G.W., and Duncan, R.A., 1989, Geologic map of the Salem 1° by 2° quadrangle, western Oregon: U.S. Geological Survey Miscellaneous Investigations Series Map I–1893, scale 1:250,000.

Wieczorek, G.F., Wilson, R.C., and Harp, E. L., 1985, Map showing slope stability during earthquakes in San Mateo County, California: U.S. Geological Survey Miscellaneous Investigations Series Map I–1257–E, scale 1:62,500.

Wilson, R.C., and Keefer, D.K., 1983, Dynamic analysis of a slope failure from the August 6, 1979, Coyote Lake, California, earthquake: Seismological Society of America Bulletin, v. 73, no. 3, p. 863–877.

———1985, Predicting areal limits of earthquake-induced landsliding, in Zioney, J.I., ed., Evaluating earthquake hazards in the Los Angeles region: An earth-science perspective: U.S. Geological Survey Professional Paper 1360, p. 317–345. □

Papers on applied geology now available as a book

An important and voluminous treatment of geologic applications in Oregon has been published in conjunction with the 40th annual meeting of the Association of Engineering Geologists held in Portland last fall:

Environmental, Groundwater, and Engineering Geology: Applications from Oregon, edited by Scott Burns of Portland State University, is a 689-page, hard-bound volume now available from the Nature of the Northwest Information Center. See listing on p. 48. □